



Pergamon

International Journal of Machine Tools & Manufacture 42 (2002) 229–236

INTERNATIONAL JOURNAL OF
**MACHINE TOOLS
& MANUFACTURE**
DESIGN, RESEARCH AND APPLICATION

Curved surface finishing with flexible abrasive tool

Sung-San Cho ^{*}, Yong-Kyoon Ryu, Seung-Young Lee

Department of Mechanical Engineering, Hongik University, 72-1 Sangsudong, Mapoku, Seoul 121-791, South Korea

Received 8 August 2000; received in revised form 5 July 2001; accepted 12 July 2001

Abstract

A flexible abrasive tool has been developed for automatic finishing of curved surfaces on three-axes machining centers. The tool is made of thermosetting polyurethane elastomer with an overcoat of aluminum oxide abrasives. The tool is capable of conducting finishing operations and deforming itself in conformity to the shape of work surface. The tool performance such as finishing capability, conformability, and durability is examined during finishing experiments on ball-end milled surfaces of high-alloyed tool steel. It is demonstrated that the tool can finish curved surfaces successfully on three-axes machining centers. The tool/work contact pressure, which influences significantly the tool performance, is analytically estimated and utilized to determine the tool path producing a constant contact pressure. It is experimentally verified that the tool path improves the finished surface roughness. © 2001 Elsevier Science Ltd. All rights reserved.

Keywords: Flexible abrasive tool; Curved surface finishing; Surface roughness; Contact analysis; Tool path

1. Introduction

Functional and aesthetic requirements in product design have increased the use of curved surfaces. Ball-end milling or electric discharge machining processes are mostly employed to produce curved surfaces, however, the machined surfaces possess irregularities due to the process characteristics such as cusps in ball-end milling and craters in electric discharge machining. Controlling the process parameters with the sacrifice of machining productivity can lessen these surface irregularities. When higher machining productivity is required and/or when the required precision of products is beyond the process capability, additional mechanical finishing operations are employed. In the case of curved surfaces, the diversity of surface shapes restricts the application of mechanized or automatic mechanical finishing processes. Since manual finishing is costly and time-consuming and the surface quality relies significantly on the worker's skill, effort has been made to develop automatic finishing systems of curved surfaces [1–6].

The most popular system substitutes robots or five-axes machining centers for human hands in manual fin-

ishing, and utilizes abrasive wheels as a finishing tool. Diverse curved surfaces can be finished in the system and the use of robots or five-axes machining centers improves the finishing efficiency. However, there are some shortcomings. First of all, the system is of high cost, and appropriate and continuous positioning of the wheel with respect to the work surface requires complex control strategies. Since relatively rigid tools are mostly used, combined effects of the tool rigidity and shape leave process-relevant irregularities on the finished surfaces. Hence, the objective of this study is to develop a finishing tool that enables automatic curved surface finishing on a three-axes machining center without complicated control techniques.

This paper is organized into three parts. The first part introduces the concept, structure, shape and manufacturing procedure of the flexible abrasive tool that is capable of conducting finishing operations and of deforming itself in conformity to the shape of the work surface. The second part contains experiment results regarding the tool performance such as finishing capability, conformability, and durability. The final part provides the tool path for improvement of the finished surface quality and experimental verification.

^{*} Corresponding author.

E-mail address: sscho@wow.hongik.ac.kr (S.-S. Cho).

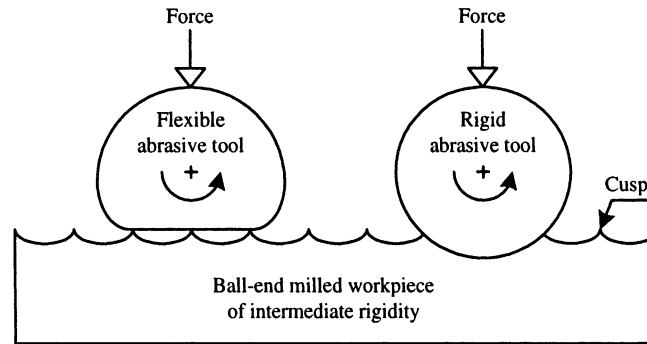


Fig. 1. Difference in abrading characteristics of flexible and rigid tools.

2. Flexible abrasive tool

The concept of a flexible abrasive tool emerges from the manual finishing in which finishing operations are performed with a flexible tool consisting of the human hand and coated abrasives. In order to clarify the concept, consider that flexible and rigid spherical abrasive tools finish a ball-end milled plane of intermediate rigidity, as shown in Fig. 1. The rigid tool removes all the interfering work material and the finished surface consists of a series of the cylindrical arced surfaces due to pick-feed of the tool. In the case of flexible tool that is ready to deform in conformity to the surface of relatively rigid work, the tool comes in contact with and removes protrusions of the milled plane. Therefore, flexible tools can finish a curved surface without altering its nominal shape.

A flexible abrasive tool has been designed on the basis of the concept mentioned above. Fig. 2 shows schematically the shape and structure of the tool. The tool has a cylindrical shape whose bottom surface is similar to a half doughnut surface. Along the cylindrical axis is provided a rectangular cross-sectional hole through which an end-part of shaft is inserted to transmit the rotational power and to mechanically clamp the tool.

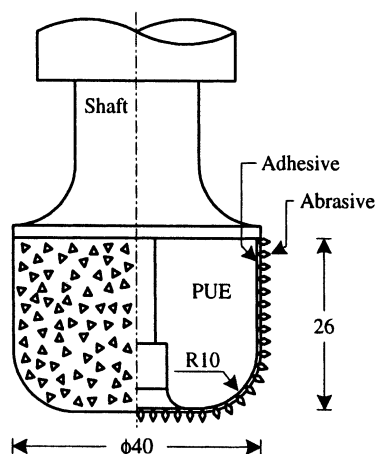


Fig. 2. Flexible abrasive tool.

Radial and axial loads acting on the tool are supported by the inserted part of the shaft and the step of the shaft contacting the upper face of the tool, respectively. The cylindrical form is made of flexible thermosetting polyurethane elastomer (PUE) with the shore durometer hardness 50 in scale A. Aluminum oxide abrasives of grit number 60 and/or 120 are glued to the surface of PUE form with a mixture of epoxy and polyamide resins. Active grit density, measured with a method similar to the soot-coated glass method, was in a range of 110–140 grits/cm². The PUE hardness was chosen with the results of preliminary tests where material removal capability and contact area were qualitatively examined for the tools with the PUE hardness 50, 70 and 90 and the grit number 60 and 120. According to the preliminary tests, the softest tool yields the largest contact area, the shallowest tool-geometry-related grooves on the finished surfaces, and the least effect of grit size on the material removal capability.

The manufacturing procedure of the flexible abrasive tool consists of the casting [7] of the PUE form and the pressure mounting [8] of abrasive grits. A mixture of the PUE reactants is poured into the mold and cured at a temperature of 200°C for 6 h. The cured PUE form is demolded and then allowed for additional curing at room temperature for a day. The surface of completely cured PUE form is abraded to remove demolding grease and to produce a rough surface, because high adhesive strength between the abrasives and the PUE surface can be achieved with the grease-free rough surface. The abraded PUE surface is coated with the adhesive resin (base binder) approximately 0.4 mm thick, and is subsequently mounted with the abrasives by rolling the PUE over the free abrasives with an appreciable pressure. The abrasive-mounted PUE is cured at room temperature for a day and then brushed to detach the loosely mounted abrasives. Finally the adhesive resin (filling binder) is applied and one-day curing is allowed. The thickness of the abrasive layer was in a range of 0.6–0.8 mm.

3. Tool performance

The flexible tool for curved surface finishing is required to possess the following capabilities: the finishing capability to effectively remove the irregularities of the work surface, conformability implying the deforming capability to conform to the shape of work surface, and durability to maintain its performance for a reasonable period of time.

The tool shape can be characterized by a circumferential surface, bottom surface and rounded corner. These three surfaces exhibit significant differences in the tool/work contact area. That is, when each tool surface is subject to a constant contact force, the circumferential and bottom surfaces yield larger contact areas and thus lower contact pressures than the corner does. Hence, the finishing capability of these three surfaces was examined individually by finishing the milled plane surfaces.

Fig. 3 shows schematically the setups for testing the finishing capability of the three surfaces. Since the test was conducted on a three-axes machining center, the work surface was inclined with 0, 45 and 90° to come in contact with the bottom, corner and circumferential surfaces, respectively. In the corner test, the finishing operation was conducted during up-travel, and the tool was pick-fed 1 mm after each up-and-down travel. In the tests of the circumferential and bottom surfaces, the work surface was finished five times without pick-feed because a single location of the work surface was repeatedly finished due to the effect of pick-feed in the corner test where the contact width in the pick-feed direction was approximately 12 mm. In the bottom surface test, the tool was fed along a zigzag path in order to make the direction of finishing velocity (circumferential velocity of the initial contact point on the surface of rotating tool) differ from the feed direction. The tests were per-

formed at a finishing speed of 33 m/min, a feed-rate of 60 mm/min, and a tool/work normal contact force of 100 N that yielded average contact pressures of approximately 0.69, 1.32 and 0.73 MPa for the bottom, corner and circumferential surfaces, respectively. The contact force was adjusted with the tool/work interference depth (tool displacement in the direction normal to the work surface at the initial contact point between tool and work surface). High-alloyed tool steel SKD-11 work surfaces were produced with ball-end milling at a tool rotational speed of 700 rpm, a feed-rate of 350 mm/min, an axial cutting depth of 1 mm, a pick-feed of 1 mm with a 10 mm-diameter mill. Roughness of ball-end milled surfaces and finished surfaces were measured with a surface profilometer, Kosaka Lab. SE-3400 and the finishing forces were measured with a tool dynamometer, Kistler 9257B. Identical tests were performed four times minimally.

Table 1 summarizes surface roughness of ball-end milled and finished surfaces in the finishing capability tests. The surface roughness was measured in the pick-feed direction. Ball-end milled surfaces of R_a 3–5 μm and R_{max} 20–27 μm are finished into surfaces of R_a 0.2–0.8 μm and R_{max} 1.3–1.8 μm . Since precision moulds generally consist of surfaces of R_{max} 2–5 μm [5], it may

Table 1
Finishing performance

Tool surface	Ball-end milled surface		Finished surface	
	R_a (μm)	R_{max} (μm)	R_a (μm)	R_{max} (μm)
Bottom	5.10	24.68	0.81	1.81
Circumference	5.04	19.94	0.23	1.29
Corner	2.94	26.85	0.21	1.61

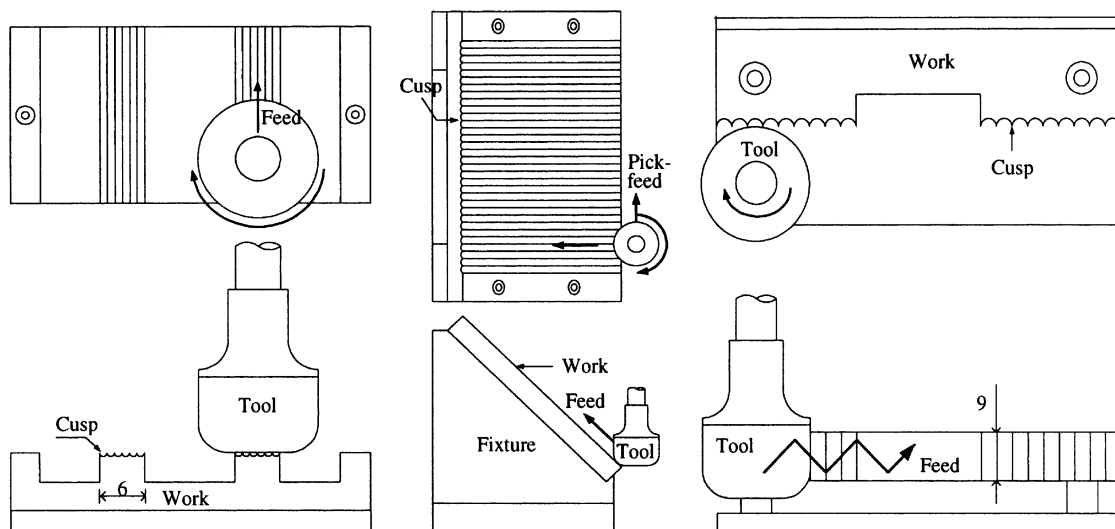


Fig. 3. Setups for finishing capability tests with bottom (left), corner (center) and circumferential (right) surfaces of flexible abrasive tool.

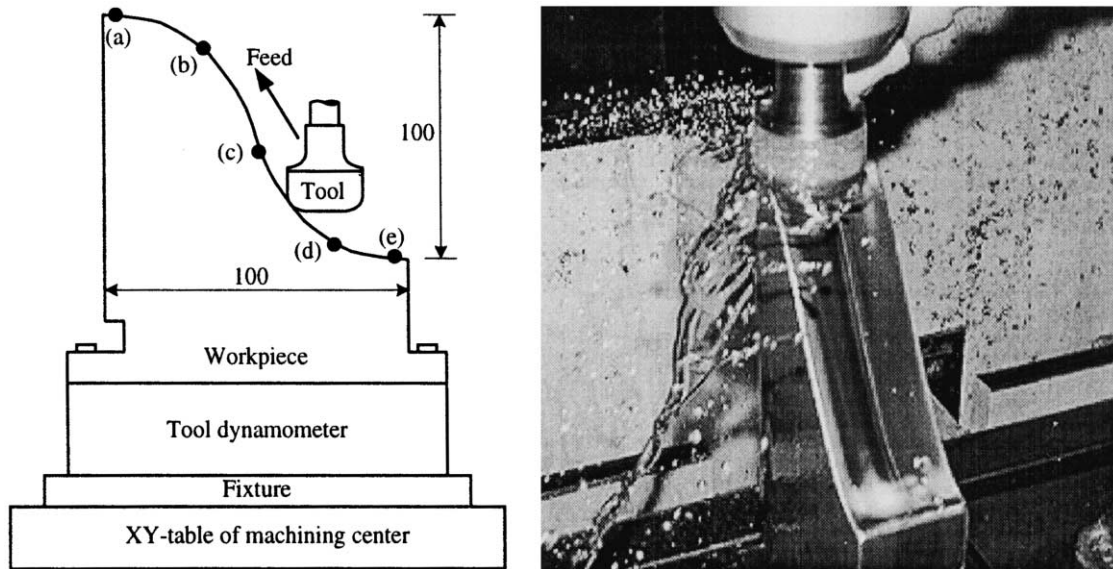


Fig. 4. Schematic representation (left) and photograph (right) of curved surface finishing.

be concluded that the finishing capability of the tool is satisfactory.

The tool conformability test was conducted for a sine curve surface, as shown in Fig. 4. Ball-end milling and finishing operations were conducted under the same conditions as those in the finishing capability test of the tool corner except that the flexible tool path maintained an interference depth of 2 mm. Finishing operations were performed twice because of the milled surface being very rough. Table 2 summarizes the surface roughness values at five characteristic locations (refer to Fig. 4) on the work surface after ball-end milling and first and second finishing. R_a and R_{max} of the milled surface range from 4.96 to 10.33 μm and from 35.55 to 92.65 μm , respectively. The milled surface roughness differs significantly due to the variation of machining capability along the cutting edge of ball-end mill. After the first finishing, the surface exhibits drastic improvement in roughness; R_a and R_{max} are in a range of 0.81–1.11 μm and 10.44–11.03 μm , respectively. The second finishing yields the surface of 0.11–0.14 μm R_a and 0.67–1.06 μm R_{max} which are considered to be satisfactory. Hence, it is concluded that the tool can perform finishing operations

successfully while it deforms its shape continuously in conformity to the curved surface. Test results show that the inclined surfaces (locations (b), (c) and (d)) are finished better than approximately horizontal surfaces (the location (a) and (e)). It is inferred that this difference is associated mainly with the roughness of the milled surface and with the contact area and pressure that are affected by the tool surface shape conducting the finishing operation.

Another important aspect of the finishing operation is to maintain accuracy of milled surfaces. Visual examination of the finished surface revealed that the pick-feed marks of the milling were still discernible on the finished surface, implying that the tool removed primarily the protrusions of the milled surface. Since the finishing depth is affected by several factors such as the interference depth, and the rotational speed and feed-rate of the tool, it may be argued that proper control of the contact and finishing conditions can provide the tool with the capability to maintain the nominal shape of the milled surface even when the interference depth is significantly greater than the milled surface roughness.

Usefulness of the flexible tool must be examined in

Table 2
Roughness of milled and finished curved surfaces

	Location	(a)	(b)	(c)	(d)	(e)
R_a (μm)	Milling	10.31	7.93	4.96	7.53	10.33
	Finishing (1st)	0.87	0.85	0.81	0.98	1.11
	Finishing (2nd)	0.13	0.11	0.12	0.10	0.14
R_{max} (μm)	Milling	59.60	68.30	35.55	92.65	67.85
	Finishing (1st)	10.98	10.83	10.44	10.91	11.03
	Finishing (2nd)	1.06	0.89	0.94	0.67	0.93

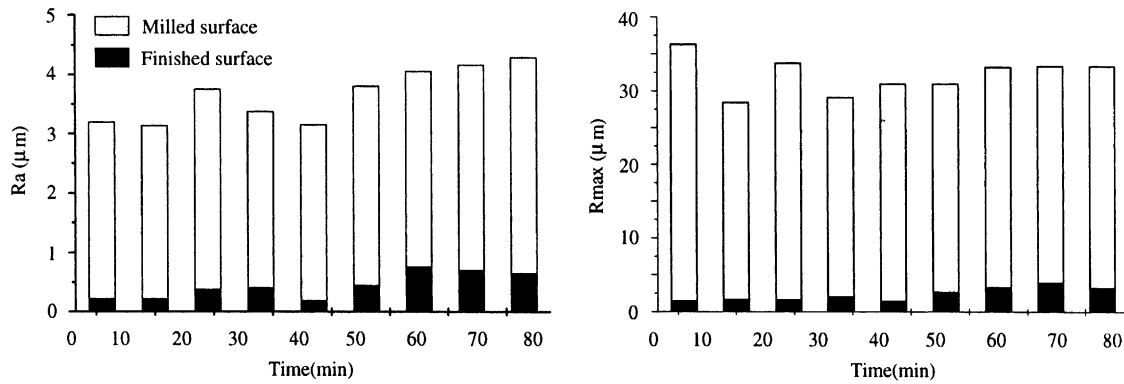


Fig. 5. Variation of surface roughness with finishing time.

terms of the durability as well. Durability of the tool is closely related with that of the tool corner because curved surfaces are primarily finished with the tool corner. Hence durability of the tool corner was tested with the setup and conditions used in the finishing capability test of the tool corner. Fig. 5 shows the variation of finished surface roughness with finishing time. The surface roughness corresponding to the finishing time up to 80 min although the test was performed for 100 min is presented. The fresh tool yields a very smooth surface and the surface roughness increases gradually with time. However, the tool used for 80 min still produces the surface that satisfies the surface roughness requirement of precision molds. Since diverse parts of the tool surface take part in curved surface finishing, and a part of the tool surface maintain its finishing capability at least for 80 min, it is anticipated that the tool life is far beyond 80 min.

Fig. 6 shows the variation of normal and finishing forces with time in the durability test. The normal force F_n is a force component perpendicular to the work surface, and the finishing force F_f is a force component in a circumferential direction of the tool. While the normal force remains unaltered as intended, the finishing force exhibiting a very large value at the beginning decreases with reduction in the decreasing rate until the finishing time of 18 min and then stabilizes into a value of 24 N.

It is inferred that the decrease in the finishing force occurs during the period when the steady-state tool/work contact geometry is established. At the beginning the entire contact surface of work possesses irregularities that need to be removed so that relatively large finishing force yields. However, the number of irregularities in the contact region diminishes with the pick-feed. This inference is confirmed with an approximate estimation that the achievement of steady-state geometry takes 18 min at a half contact width of 6 mm in the pick-feed direction, a pick-feed of 1 mm, and a finishing time of 3 min between two successive pick-feeds.

4. Tool path

When the tool moves along the path of constant interference depth in curved surface finishing, the contact pressure and area vary depending on the shape of work surface. The contact pressure affects the penetration depth of abrasives into the work surface while the contact area in conjunction with the pick-feed influences the number of contacts that a single location on the work surface is subject to. Hence, the finished surface roughness, as evidenced in Table 2, depends on the contact condition. Moreover, it is expected that the curved surface finishing along the path of constant contact pressure can make the finished surface roughness more uniform.

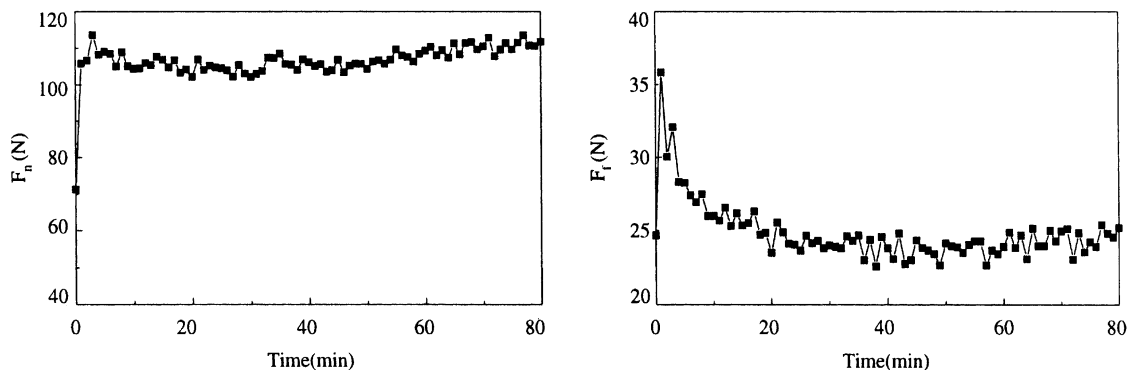


Fig. 6. Variation of finishing forces with time during durability test.

Fig. 7 shows the algorithm to generate the tool path of constant contact pressure. The algorithm requires information of geometries and mechanical properties of the tool and work, a desired contact pressure at initial contact points, a candidate interference depth, and some auxiliary data. A series of initial contact points on the work surface is generated first, the corresponding initial contact points on the tool surface is determined, and then the gap distance is estimated in terms of coordinates in the cotangent plane in the configuration that the corresponding initial contact points coincide. The tool approaches the work surface with a distance of candidate interference depth in the normal direction, and then an intersection curve between the tool and work surfaces is estimated. The region enclosed by the intersection curve, a candidate contact region, is divided into smaller rectangular cells. The pressure in the candidate contact region is estimated using the non-Hertzian closely conforming elastic contact theory [9]. The cells subject to negative pressure are eliminated from the candidate contact region and the analysis is repeated with the modified

contact region until no negative pressure occurs in the region. With the completion of the contact analysis, the pressure at the initial contact point is compared with the desired pressure. If the desired pressure is not obtained, the contact analysis procedure is repeated with a modified interference depth until the desired pressure is obtained. The tool position is calculated with the initial contact point on the work surface, the tool geometry and the interference depth. The above procedure is repeated at a series of initial contact points, and the tool path is generated by linearly connecting a series of tool positions.

The algorithm requires elastic modulus and Poisson's ratio of the tool. Elastic modulus of the tool was measured semi-experimentally because of the absence of any available standard method. The tool attached to the spindle of machining center was compressed in the normal direction against a 45°-inclined polished plane surface, and then the contact forces were measured with the tool dynamometer to estimate the normal contact force. After that, the tool was rotated for 20 s to abrade the

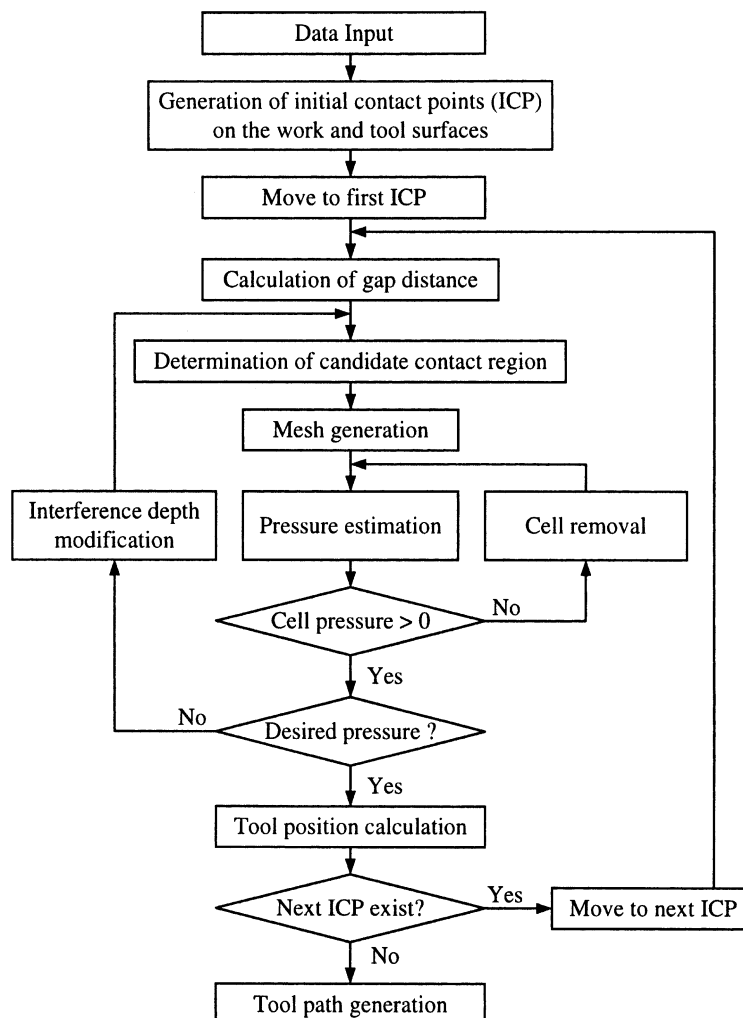


Fig. 7. Tool path generation algorithm for constant contact pressure.

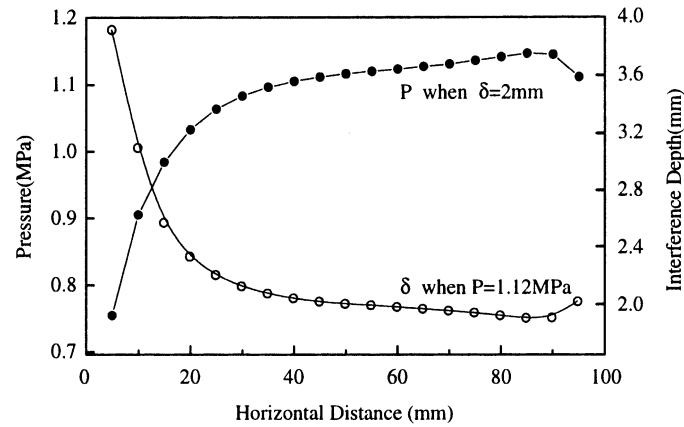


Fig. 8. Variation of maximum contact pressure (P) and interference depth (δ) along sine curve surface when $\delta=2$ mm and $P=1.12$ MPa, respectively

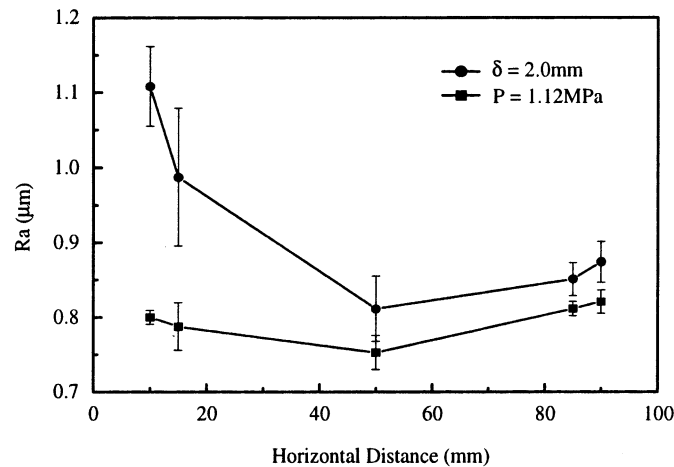


Fig. 9. Roughness of surfaces finished at a contact pressure of 1.12 MPa and at an interference depth of 2.0 mm

surface, and then the major and minor axes of the elliptical abraded region (presumably the contact region) were measured. This contact problem was analyzed using the algorithm with assumptions that the tool is homogeneous and possesses Poisson's ratio 0.48, a typical value of the PUE [7]. The analysis was repeated with various values of elastic modulus until the analysis yielded the normal contact force and contact region similar to the measured ones. The measurement and analysis were conducted at interference depths of 1, 2, 3 and 4 mm. The elastic modulus of the tool was estimated to be 3.5 MPa.

Fig. 8 shows an analysis result of contact between the tool and the sine curve surface. The elastic modulus and Poisson's ratio of the work were assumed to be 200 GPa and 0.33, respectively. The curve with dark symbols represents the contact pressure at a series of initial contact points when the tool path maintains an interference depth of 2 mm. In the regions where work surface is almost horizontal and/or concave (near the locations (d) and (e) in Table 2), the tool path of constant interference depth produces relatively low contact pressure, and thus the increase in the interference depth is required to produce a

constant contact pressure. The curve with open symbols represents the tool/work interference depth that produces a contact pressure of 1.12 MPa along the tool path. The contact pressure of 1.12 MPa corresponds to the pressure at a horizontal distance of 50 mm on the pressure curve.

Fig. 9 shows measured roughness values at five locations on the sine curve surfaces finished along the tool paths of interference depth 2 mm and of contact pressure 1.12 MPa. The tool path of constant contact pressure lessens the variation of surface roughness along the work surface. Moreover, the overall reduction in the average and standard deviation of surface roughness values is achieved. Hence, it is concluded that the tool path of constant contact pressure is more efficient than that of constant interference depth.

5. Conclusions

A flexible abrasive tool has been developed for automatic finishing of curved surfaces on three-axes machining centers, and the tool performance has been exper-

imentally examined. The tool path of constant contact pressure has been analytically determined and its usefulness has been experimentally examined.

The flexible tool finishes curved surfaces successfully on three-axes machining centers without altering the pre-machined work surface shape. The tool maintains its finishing capability for more than 80 min. The tool path of constant contact pressure improves the quality of the finished surface compared with that of constant interference depth.

Acknowledgements

This work was supported by grant No. 981-1007-047-2 from the Basic Research program of the Korea Science and Engineering Foundation.

References

- [1] M. Kunieda, T. Nakagawa, T. Higuchi, *JSPE* 54 (1988) 125.
- [2] K. Kamijyo, M. Sakamoto, T. Asao, Y. Takeuchi, *JSME(C)* 55 (1989) 193.
- [3] K. Kamijyo, Y. Mizugaki, M. Sakamoto, *JSME(C)* 57 (1991) 1019.
- [4] S. Kamezaki, T. Aoyama, I. Inasaki, *JSME(C)* 57 (1991) 3714.
- [5] M.C. Lee, D.J. Ha, *KSPE* 16 (4) (1999) 163.
- [6] J. Zhao, K. Saito, T. Kondo, H. Narahara, S. Igarashi, T. Sasaki, L. Zhang, *Int. J. Mach. Tools Manufact.* 35 (1995) 1683.
- [7] S.S. Schwartz, S.H. Goodman, *Plastics Materials and Processes*, Van Nostrand Reinhold, New York, 1986 (376-395).
- [8] J.A. Borkowski, A.M. Szymanski, *Uses of Abrasives and Abrasive Tools*, Ellis Horwood, New York, 1992 (42-48).
- [9] B. Paul, J. Hasheni, *J. Appl. Mech.* 48 (1981) 543.